Chalcogenide Letters Vol. 16, No. 7, July 2019, p. 351 - 356

ANNEALING IMPACT ON STRUCTURAL, MORPHOLOGICAL AND TOPOLOGICAL PROPERTIES OF THERMALLY EVAPORATED Cu_2SnS_3 AND Cu_3SnS_4 THIN FILMS

B. Y. TAHER[a], M. F.A. ALIAS[b*], I. S. NAJI[b], A. A. ALNAJJAR[c]
[a]*College of Agriculture, University of Anbar, Iraq*
[b]*Department of Physics, College of Science, University of Baghdad, Baghdad, Iraq*
[c]*Arab Science and Technology Foundation, Sharjah, UAE*

Nano-powder was used to prepare both Cu_2SnS_3 and Cu_3SnS_4 thin films by thermal evaporation technique under 10^{-5} Torr on glass and Si substrates as deposited and annealed at 523 K for 30 minute with thickness 400±5nm and 350 ±5nm respectively. Structural, morphological and Topology properties have been investigated by using X-ray diffraction (XRD), Raman spectroscopy, scanning electron microscopy (SEM) and atomic force microscopy (AFM), respectively. XRD results showed that all prepared films have amorphous structure. Raman spectra analysis found two peaks for all prepared specimens at 521 cm^{-1} and 303 cm^{-1} which correspond to Si substrate and cubic structure of Cu_2SnS_3, respectively. Micro Raman images illustrated the area completely covered only with Cu_2SnS_3 surface crystals for Cu_2SnS_3 and Cu_3SnS_4 thin films as deposited, whereas for prepared annealed thin films showed the droplet liquid phase more than as deposited specimens. Morphological results showed the prepared annealed thin films have less porosity with enhanced microstructure compared with that as deposited specimens. AFM images showed the grain size and roughness average decreased for annealed Cu_2SnS_3 thin film, while increased for annealed Cu_3SnS_4 thin films, All AFM images exhibit smooth, cover the substrate, regular structure and homogenous surfaces have morphological characterized by tubes shaped grains together in big clusters. All samples as deposited and annealed varied in surface roughness average (0.385 – 1.85) nm, root mean square (0.486-2.1) and average grain sizes in the range of (35.28 – 43.65) nm.

(Received April 26, 2019; Accepted July 25, 2019)

Keywords: Copper-tin-sulphide, Cu_2SnS_3 and Cu_3SnS_4 thin films, Thermal evaporation, annealing impact, AFM, SEM, Raman

1. Introduction

The importance of study topographical and morphological properties come from the coatings surface morphology reflects the microstructure of underlying bulk material can act as a fingerprint for each type, the development of nanomaterials with special size and shape may lead to new chances to explore material, physical and chemical properties [1-3].The morphology of the absorber layer Cu_2SnS_3 have been studied [4-6]. The prepared films had a much less compact structure, homogenously distributed over the whole surface area of the sample and had large grains of between 2 and 6 μm in diameter can be observed with pinholes of similar horizontal dimensions. The atomic force microscopy (AFM) image of thin Cu_2SnS_3 film has been studied and showed that these types of samples have an unusual morphology characterized by sheet-shaped grains grouped together in big clusters with sizes varying in the range of 1×0.4 μm and 2.5×1.4 μm [7-10]. Morphological characterizations of Cu_3SnS_4 were founded by many researches by scan electron microscopy (SEM) or transition electron microscopy (TEM) techniques where, SEM images showed that samples contain 1 μm of pores [11]. Cu_3SnS_4 have been prepared with nanoshell tubes [12]. Raman spectroscopy offers an alternative to detect the phases which have

*Corresponding author: may20131313@yahoo.com

similar structure because of the differences in the phonon spectra from these compounds[13]. Raman spectroscopy was used by several research groups to find the Raman peak shift to detect the secondary phases, structure type and crystallinity for prepared thin films, where the extent of crystallinity or non crystallinity detected by the X-ray diffraction technique which reflected in the Raman spectra of the thin films as well as. The bands are broad in the amorphous materials and sharp in the crystalline materials[14]. Raman peak shifted for cubic phase were reported at 303 cm^{-1}, 355 cm^{-1}[15],303 cm^{-1} [16],267 cm^{-1}, 303 cm^{-1}, 356 cm^{-1} [17,18].

This study focused on effect the annealing temperature on the structural, morphology and topology properties of Cu_2SnS_3 and Cu_3SnS_4 thin films prepared by thermal evaporation technique.

2. Expermental

In this study, firstly we prepared Cu_2SnS_3 and Cu_3SnS_4 thin films on glass and Si substrates by thermal evaporation technique from their nanopowders which have been prepared by chemical bath deposition (CBD) technique as described earlier [3,4,8,19,20]. Silicon n-type with thickness 508 μm, resistivity 0.015 Ω.cm and concentration 3.9×10^{19} cm^{-3} have been cleaned and used to prepare thin films. The process for obtaining the powder start after finishing from prepared thin films by chemical bath deposition technique at the optimum prepared conditions such as substrate temperature = 343 K, pH = 2, and deposition time = 80 minute) for Cu_2SnS_3 and at substrate temperature = 313 K, pH = 1.5, and deposition time = 80 minute for Cu_3SnS_4. The nanosolution was candidate followed by wished in distilled water and acetone for several times, and finally placed in oven at 373 K for 120 minute. The nanopowder was then cooled to room temperature with approximately the same rate as the heating rate. The prepared conditions for thermal evaporation technique were included vacuum pressure (3×10^{-5}) Torr. The time of evaporation is 3.00 min. for Cu_2SnS_3 and 4.16 min. for Cu_3SnS_4. The prepared samples for Cu_2SnS_3 and Cu_3SnS_4 were annealed at 523 K for 30 min. with annealing rate 275.72 K/min. and cooling rate 274.00 K/min. by using vacuum oven. The film thickness was calculated from the following equation $m = 2 \times \pi \times d \times Z^2 \times t$, where, m is mass of powder, π is constant ratio, d is density of compound, Z is distance from the boat to the edge of substrate = 15 cm, t is thickness of required film.

The crystalline structures of the nanopowder of Cu_2SnS_3 and Cu_3SnS_4 were characterized [10] using X-ray diffraction (XRD) with Cu K_α radiation (λ = 1.54060 Å), where operated in the range of 2θ degree from 20° to 60° using step size of 0.05° and step time of 0.60 s. Working voltage and acceleration current were 40 kV and 30 mA, respectively. The structural features were studied by Raman microscope spectrometer, model (Senterra, Bruker, Germany), with micrograph pictures with the excitation wavelength from an argon ion laser which was 514.5 nm at 20 mW. The morphological features were measured by scanning electron microscopy (SEM) model (Inspect S50) with accelerating voltage 200V to 30 kV, probe current 1pA to 2 μA with high resolution mode. The topological analysis was investigated by using atomic force microscope (AFM), model (SPM), where films surface topography and image size are observed approximately from (1957, 2001) to (5097, 5073) nm with (484,495) to (508,505) pixels by scanning probe microscope (SPM). The symbols of prepared samples a and b for Cu_2SnS_3 as deposited and annealed, whereas, c and d for Cu_3SnS_4 thin films samples as deposited and annealed respectively.

3. Results and discussion

Structural properties of Cu_2SnS_3 and Cu_3SnS_4 thin films as deposited and annealed at 523 K for 30 min. on glass substrate showed amorphous structure. This may be due to amorphous glass substrate and low thickness of prepared thin films [21].

Cu_2SnS_3 and Cu_3SnS_4 thin films as deposited and annealed at 523 K for 30 min. were deposited on Si substrates were characterized by Raman spectroscopy. Raman spectra of prepared

thin films were showed in Fig. 1. The peaks were found at 521 cm^{-1} which correspond to Si substrate, and other peaks were found at 303 cm^{-1} for all Cu_2SnS_3 and Cu_3SnS_4 thin films as deposited and annealed. These peaks correspond to cubic Cu_2SnS_3. The secondary phases were not found in any of these samples. The presence cubic phase agrees with that found by previous researchers[14,22]. The peak intensity of prepared thin films was smaller than that of Si substrate, because the prepared thin films have very thinner thickness than that of Si substrate which has high intensity. The cubic structure for the films may be due to the structure of Si substrate which is cubic with (111) miller indices, therefore the nanopowder of Cu_2SnS_3 and Cu_3SnS_4 were deposited on the crystalline Si substrate and has same structure shape of substrate. The peaks of prepared thin films are broad due to have small thickness compared with Si substrate which has sharp peak [14] as we mentioned previously. The broad peak of prepared thin films phase refers to presence quantum confinement effect due to low intensity of Raman spectra and broad of peak band [23].

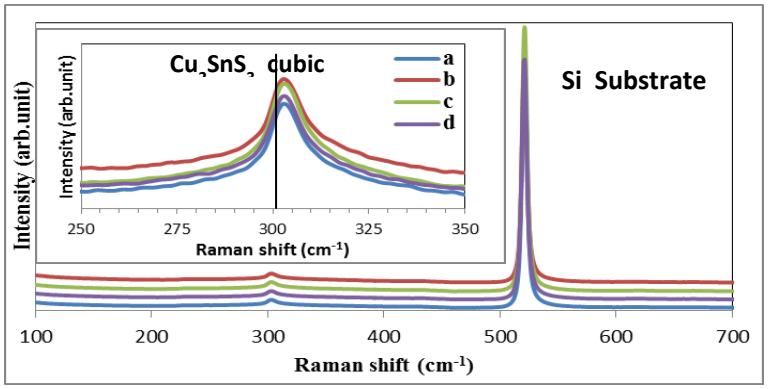

Fig. 1. Raman spectra of (a) Cu_2SnS_3 as deposited (b),annealed Cu_2SnS_3 ,(c) Cu_3SnS_4 as deposited (d) annealed Cu_3SnS_4on silicon substrates.

Micro Raman images for all devices were shown in Fig. 2, where the area completely covered only with Cu_2SnS_3 surface crystals for Cu_2SnS_3 and Cu_3SnS_4 as deposited. The effect of annealing in prepared thin films showed the droplet liquid phase more than the samples without annealing because effect the temperature on the crystals.

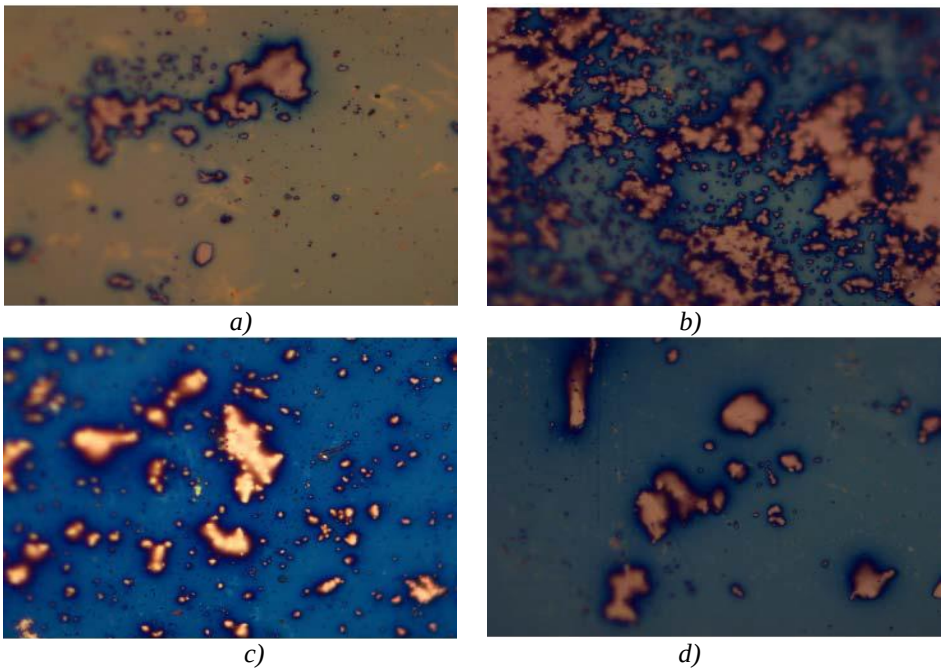

Fig.2. Chemical Micro-Raman images of: (a) Cu_2SnS_3 as deposited, (b) annealed Cu_2SnS_3, (c)Cu_3SnS_4 as deposited (d) annealed Cu_3SnS_4

Morphological properties of Cu_2SnS_3 and Cu_3SnS_4 thin films were measured by scanning electron microscopy (SEM). SEM pictures for samples as deposited and annealed at 523 K for 30 min. for both Cu_2SnS_3 and Cu_3SnS_4 thin films were deposited on Si substrates were shown in figures 3 and 4, respectively. Cu_2SnS_3 and Cu_3SnS_4 thin films as deposited have more porosity compared with that annealed. Cu_2SnS_3 thin film as deposited had medium crystals covering large region of total film with enhanced microstructure, but annealed Cu_2SnS_3 thin film had small crystals covering large region of total film, while for Cu_3SnS_4 thin film as deposited produced agglomerate particle with large crystal covering limited region of total film, whereas annealed Cu_3SnS_4 thin film produced agglomerate particles with large crystals covering almost region of total film with enhanced microstructure.

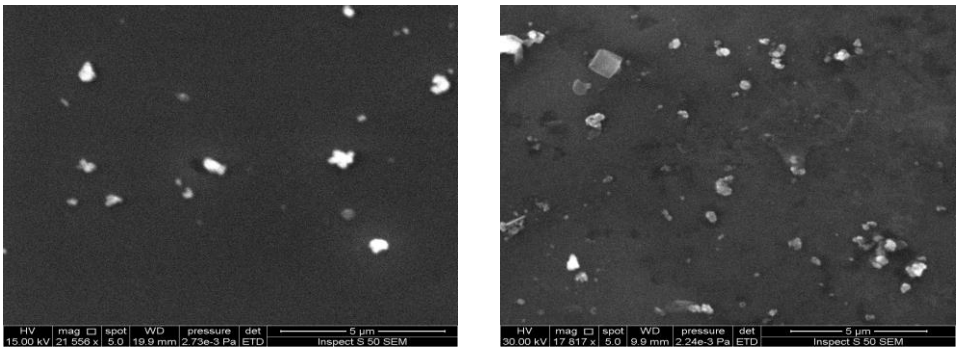

a) 5µm *b) 5µm*

Fig.3. SEM pictures of Cu_2SnS_3 thin films (a) as deposited (b) annealed.

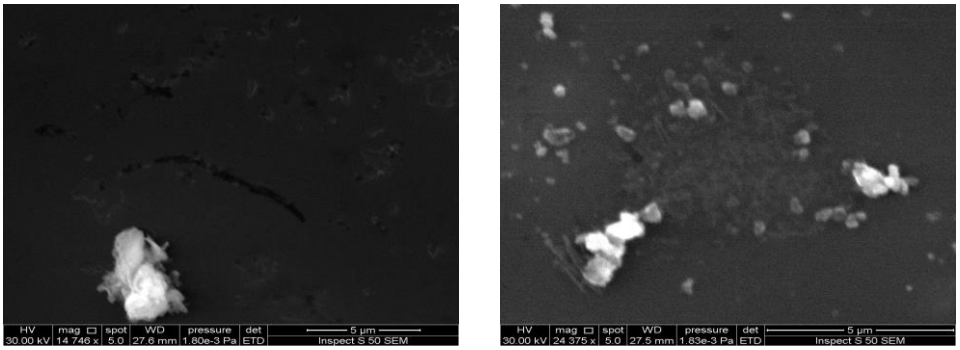

a) 5µm *b) 5µm*

Fig. 4. SEM pictures of Cu_3SnS_4 thin films (a) as deposited and (b) annealed.

Topography studies were done by using atomic force microscopy. AFM images for samples as deposited and annealed at 523 K for 30 min. for both Cu_2SnS_3 and Cu_3SnS_4 thin films deposited on glass substrates were shown in figures 5 and 6, respectively. Values of average grain size, surface roughness and root mean square for Cu_2SnS_3 and Cu_3SnS_4 thin films were shown in Table 1.

All AFM images exhibit smooth, cover the substrate in good way, regular structure and homogenous surfaces have morphological characterized by tubes shaped grains together in big clusters. All samples as deposited and annealed varied in surface roughness average (0.385 – 1.85 nm), root mean square (0.486-2.1) and average grain sizes in the range of (35.28 – 43.65 nm).

The grain size and roughness average decreased for annealed Cu_2SnS_3 thin film, whereas increased for annealed Cu_3SnS_4 thin films. This may be due to agglomerate particles occurred due to non-dispersion of the particle or may have porosity [24, 25]. All samples have uniform films and small roughness; also particles in nanometer dimension and it has non porous structure.

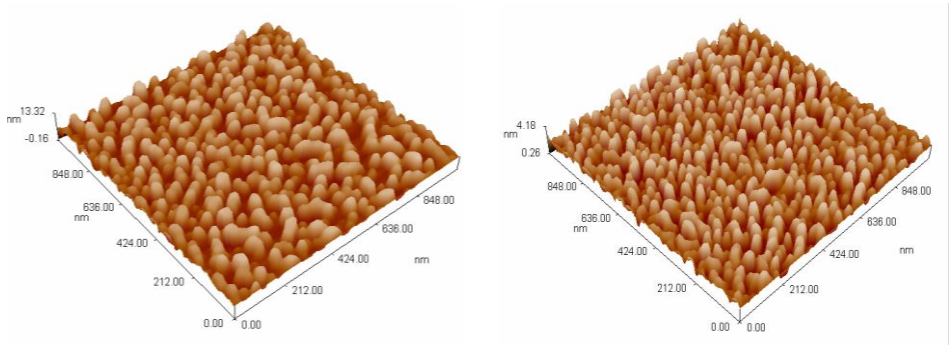

a) *b)*

Fig. 5. AFM images of Cu_2SnS_3 thin films (a) as deposited (b) annealed.

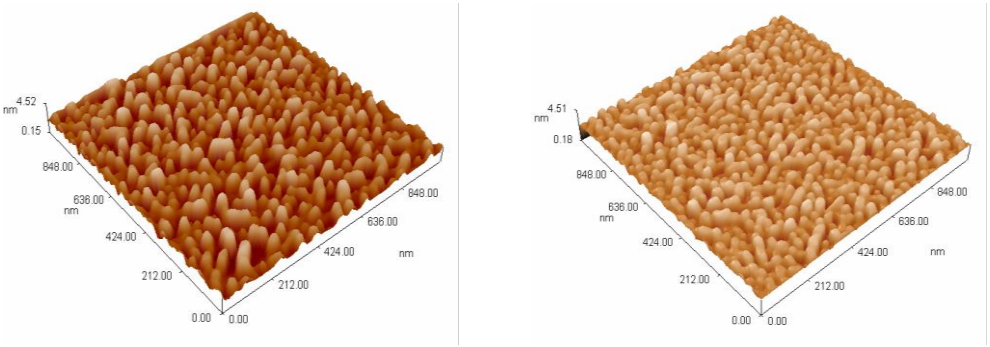

a) *b)*

Fig. 6. AFM images of Cu_3SnS_4 thin films (a) as deposited (b) annealed.

Table 1. Topological characteristics of Cu_2SnS_3 and Cu_3SnS_4 thin films as deposited and annealing.

Symbol	Thin film name	Average grain size(nm)	Roughness average (nm)	Root mean square (nm)
a	**Cu_2SnS_3** as deposited	43.65	1.850	2.100
b	**Cu_2SnS_3** as annealing	35.28	0.617	0.711
c	**Cu_3SnS_4** as deposited	35.85	0.385	0.486
d	**Cu_3SnS_4** as annealing	39.24	0.596	0.703

4. Conclusions

Nanopowder was used to prepare Cu_2SnS_3 and Cu_3SnS_4 thin films on glass and Si substrates as deposited and annealed at 523 K for 30 minute with 350 and 400 nm thickness using thermal evaporation technique. Structural analysis showed all prepared films as deposited and annealed on glass substrates have amorphous structure. Raman analysis illustrated the peaks were founded at wave number 521 cm^{-1} and 303 cm^{-1} which correspond to Si substrate and cubic structure of Cu_2SnS_3 for all prepared thin films, respectively. SEM images showed thin films as deposited have more porosity compared with that annealing. All AFM images exhibit smooth, cover the substrate in good way, regular structure and homogenous surfaces have morphological characterized by tubes shaped grains together in big clusters. Grain size and roughness average decreased at annealing for Cu_2SnS_3 thin film, whereas increased for annealed Cu_3SnS_4 thin films.

References

[1] H. Dahman, S. Rabaoui, A. Alyamani, L. El Mir, Vacuum **101**, 208 (2014).
[2] D. Tiwari, T. K. Chaudhuri, T. Shripathi, U. Deshpande, R. Rawat, Solar Energy Materials and Solar Cells **113**, 165 (2013).
[3] M. F. A. Alias, I. S. Naji, B. Y. Taher, International Journal of Electrical Engineering **2**(12), 1 (2014).
[4] I. S. Naji, M. F. A. Alias, B. Y. Taher, A. A. J. Al-Douri, Chalcogenide Letters **15**(2), 83 (2018).
[5] D. M. Berg, R. Djemour, L. Gütay, G. Zoppi, S. Siebentritt, P. J. Dale, Thin Solid Films **520**(19), 6291 (2012).
[6] M. H. Sayed, E. V. C. Robert, P. J. Dale, L. Gütay, Thin Solid Films **669**, 436 (2019).
[7] R. A. Becerra, J. M. Correa, H. Suarez, G. Gordillo, Journal of Physics: Conference Series **480**(1), 12008 (2014).
[8] B. Y. Taher, M. F. A. Alias, I. S. Naji, H. Alawadhi, A. A. J. Al-Douri, Australian Journal of Basic and Applied Sciences **9**(20), 406 (2015).
[9] I. S. Naji, M. F. A. Alias, B. Y. Taher, Australian Journal of Basic and Applied Sciences **9**(23), 547 (2015).
[10] M. F. A. Alias, I. S. Naji, B. Y. Taher, A. A. J. Al-Douri, Journal of Non- Oxide Glasses **8**(4), 93 (2016).
[11] Y. Goto, Y. Sakai, Y. Kamihara, M. Matoba, Japanese Journal of Applied Physics **54**(2), (2015).
[12] H. Hu, Z. Liu, B. Yang, X. Chen, Y. Qian, Journal of Crystal Growth **284**(1–2), 226 (2005).
[13] D. M. Berg, R. Djemour, L. Gütay, S. Siebentritt, P. J. Dale, X. Fontane, V. Izquierdo-Roca, A. Pérez-Rodriguez, Applied Physics Letters **100**(19), (2012).
[14] B. Minceva-Sukarova, M. Najdoski, I. Grozdanov, C. J. Chunnilall, Journal of Molecular Structure (1997), p. 267.
[15] P. A. Fernandes, P. M. P. Salomé, A. F. D. Cunha, Journal of Physics D: Applied Physics **43**(21), (2010).
[16] J. Kavalakkatt, S. Levcenko, M. C. Lux-Steiner, K. Kornhuber, X. Lin, A. Ennaoui, Thin Solid Films **535**, 10 (2013).
[17] P. A. Fernandes, P. M. P. Salomé, A. F. da Cunha, Thin Solid Films **517**(7), 2519 (2009).
[18] S. R. Kodigala, Thin Film Solar Cells from Earth Abundant Materials: Growth and Characterization of Cu2ZnSn(SSe)4 Thin Films and Their Solar Cells (Elsevier, 2014).
[19] A. C. Lokhande, R. B. V. Chalapathy, M. He, E. Jo, M. Gang, S. A. Pawar, C. D. Lokhande, J. H. Kim, Solar Energy Materials and Solar Cells **153**, (2016).
[20] J. Y. Park, R. B. V. Chalapathy, A. C. Lokhande, C. W. Hong, J. H. Kim, Journal of Alloys and Compounds **695**, 2652 (2017).
[21] B. G. R. Sharma Bisen, D. P. Shukla, Usha, Sharma, Recent Research in Science and Technology **4**(8), 77 (2012).
[22] A. Safdar, M. Islam, I. Ahmad, A. Akram, M. Mujahid, Y. Khalid, Y. Zhu, Materials Science in Semiconductor Processing **41**, 420 (2016).
[23] O. P. Singh, N. Muhunthan, V. N. Singh, B. P. Singh, Advanced Materials Letters **6**(1), 2 (2015).
[24] S. Gorer, G. Hodes, Journal of Physical Chemistry **98**(20), 5338 (1994).
[25] V. Maheskumar, P. Gnanaprakasam, T. Selvaraju, B. Vidhya, Journal of Electroanalytical Chemistry **826**, 38 (2018).